Energy, Volume 102, 1 May 2016, Pages 343-353
DOI:10.1016/j.energy.2016.02.079

Calcium looping with supercritical CO_2 cycle for decarbonisation of coal-fired power plant

Dawid P. Hanak*, Vasilije Manovic

Energy, 102, 343–353

Combustion and CCS Centre, Cranfield University,

Bedford, Bedfordshire, MK43 0AL, UK

Corresponding author*: Dawid Hanak

d.p.hanak@cranfield.ac.uk

Calcium looping with supercritical CO_2 cycle for decarbonisation of coal-fired power plant

Dawid P. Hanak, Vasilije Manovic*

Combustion and CCS Centre, Cranfield University, Bedford, Bedfordshire, MK43 0AL, UK

**d.p.hanak@cranfield.ac.uk*

Abstract

State-of-the-art integration scenarios of calcium looping (CaL), which is an emerging CO_2 capture technology, assume that excess heat is used to raise steam for the steam cycle and result in a net efficiency penalty of 6.0–8.0% points. In this study, a concept using the supercritical CO_2 cycle (s-CO_2) instead of the conventional steam cycle is proposed. Retrofit of CaL with recompression s-CO_2 cycle to the 580 MW_{el} coal-fired power plant was found to result in a net efficiency penalty of 6.9%$_{HHV}$ points. This is 1%$_{HHV}$ point lower than that for the same system linked with the steam cycle having the same turbine inlet conditions (593.3°C/242.3 bar). A further reduction of the net efficiency penalty to 5.8%$_{HHV}$ points was achieved through considering a pump instead of a first CO_2 compression stage and increasing the turbine inlet temperature to 620°C and pressure to 300 bar. As the s-CO_2 cycle's specific capital cost is up to 27% lower than that of the equivalent steam cycle, CaL with s-CO_2 cycle is a viable option for the coal-fired power plant decarbonisation. Moreover, it can be expected that this cycle can be successfully implemented in other high-temperature looping cycles, such as chemical looping combustion.

Key Words: Calcium looping, carbon capture, coal-fired power plant, supercritical CO_2 cycle, recompression Brayton cycle, efficiency penalty reduction

1 INTRODUCTION

The power generation sector is one of the key sectors that need to be decarbonised by 2050 to meet the greenhouse gas emission reduction target and to mitigate drastic climate change [1–4]. It has been predicted that its near-complete decarbonisation would account for approximately 28% of the total CO_2 emission reduction in 2025 [5]. Regardless of that, coal-fired power plants are currently responsible for more than 70% of the total CO_2 emissions from the power sector and their share in the energy portfolio is predicted to decrease only by around 6%, for example, from around 40% [5,6] in 2013 to 34% in 2040 [6]. On the other hand, a 5% increase in the renewable energy sources share is predicted within this time frame [6]. Yet, large-scale deployment of renewables requires more backup capacity to make up for their intermittency, introducing additional costs. As a result, coal-based power generation remains more attractive for investors and is expected to remain the key power source in the future energy portfolio [7]. Therefore, carbon capture and storage (CCS) is expected to act, at least, as a bridge to the clean power generation future [8].

Regardless of the recent progress in oxy-combustion and chemical solvent scrubbing post-combustion CO_2 capture technologies [9,10], the efficiency penalty associated with integration of these systems to coal-fired power plants is predicted to be 7.0–12.5% points [11–16], which would increase the cost of electricity by at least 60% [17–20]. Therefore, emerging technologies, which offer more competitive performance of the retrofitted system, are being developed [21]. Calcium looping (CaL), which is based on the reversible carbonation reaction of lime, has been proposed as a viable and efficient process for decarbonisation of coal-fired power plants [22]. A recent review [23] revealed that the efficiency penalty associated with CaL is projected to be within 6.0–8.0% points, depending on the level of heat integration. The main reason

behind the superior performance of CaL compared to the more mature CO_2 capture technologies, is its high-temperature operation and high-grade heat availability [22,24,25].

The state-of-the-art CaL integration scenarios assume that high-grade heat is recovered to generate steam at a high pressure, which is then used to generate power in the conventional steam cycle based on the Rankine cycle. Yet, it is worth highlighting that CaL operates within the temperature range of 600–950°C [23], which is similar to the operating temperatures of the natural gas turbine bottoming cycle (600°C) [26], high-temperature gas-cooled nuclear reactors (850–1000°C) [27], sodium-cooled fast nuclear reactors (500–550°C) [28,29], helium-cooled fusion nuclear reactors (500°C) [30] and concentrating solar power plants (800–900°C) [31,32] – technologies for which alternative thermodynamic cycles, such as the Brayton cycle using He or supercritical CO_2 (s-CO_2), have been investigated.

Compared to the conventional supercritical steam cycle based on the Rankine cycle, the He and s-CO_2 cycles can achieve higher cycle efficiencies that can be as high as 50-60%, depending on the turbine inlet conditions and the cycle architecture [31–34]. Dostal et al. [34] have shown that the s-CO_2 cycle outperforms the equivalent He cycle at the same turbine inlet temperature. This is mostly because of near-critical-point operation of the CO_2 compressors resulting in the compression power requirement being only around 30% of the turbine power output. Also, due to the high density and low heat capacity of supercritical CO_2, the size of the turbomachinery is considerably smaller than that for the steam cycle and the He cycle. In addition, the layout of the system based on the Brayton cycle is simpler than that for the steam cycle [34–37]. All of these features of the s-CO_2 cycle are reflected in the specific capital cost ($/$MW_{el}$), which for this cycle has been estimated to be up to 27% lower than for the

superheated steam cycle and 11% lower than the equivalent He cycle [34], making the s-CO_2 cycle a technically and economically viable option for future power generation systems. This is also reflected in a wide spectrum of investigated applications of the s-CO_2 cycle that vary from low-grade waste heat recovery systems [38], fuel cell hybrid systems [39] and liquefied natural gas power and refrigeration systems [40,41], through to solar [31,32,42], nuclear [27–30,34,38,43] and even coal-fired power plants [44]. The aforementioned qualities make the s-CO_2 cycle worth considering as an alternative to the conventional Rankine steam cycle [35].

Reduction of the efficiency and economic penalties associated with CO_2 capture is required for the industrial deployment of these technologies. CaL, as an emerging CO_2 capture technology, has already been proven as a viable alternative to mature technologies for decarbonisation of coal-fired power plants. Yet, the state-of-the-art integration scenarios suggest that the excess high-grade heat from the CaL plant can be utilised in the primary or the secondary steam cycle for power generation [23]. Due to higher cycle efficiency and lower specific capital cost associated with the s-CO_2 cycle compared to the steam cycle, the concept of the CaL plant with s-CO_2 cycle for decarbonisation of a coal-fired power plant is proposed in this study. For the purpose of this study, the s-CO_2 process model was developed and then adapted to the existing CaL process model [45]. The performance of the proposed retrofit scenario is first compared with the CaL plant with the supercritical reheated steam cycle reported by Hanak et al. [45]. Then, the impact of variations of the s-CO_2 hardware and the turbine inlet conditions on the net thermal efficiency of the retrofitted system are investigated. Finally, the optimum design is proposed based on sensitivity studies and further improvements in the retrofitted system performance are identified.

2 PROCESS MODEL DEVELOPMENT

2.1 Process description

This study analyses a scenario in which the CaL plant, which comprises two interconnected fluidised bed reactors operating at atmospheric pressure, is retrofitted to a 580 MW_{el} coal-fired power plant to achieve a total CO_2 capture level of 90%. In this system, CO_2 from the flue gas is removed in the carbonator, which operates at 650°C, through the exothermic reaction with CaO. The saturated sorbent ($CaCO_3$) is then regenerated at a high temperature (900°C) in the calciner, which is ensured through oxy-combustion of coal. The high-temperature operation of the CaL plant allows for high-grade heat recovery from the carbonator and the process streams. The high-grade heat is utilised to generate an additional amount of power in the s-CO_2 cycle, which is evaluated in this study as an alternative to the supercritical steam cycle considered thus far in the literature [22–24,46–53].

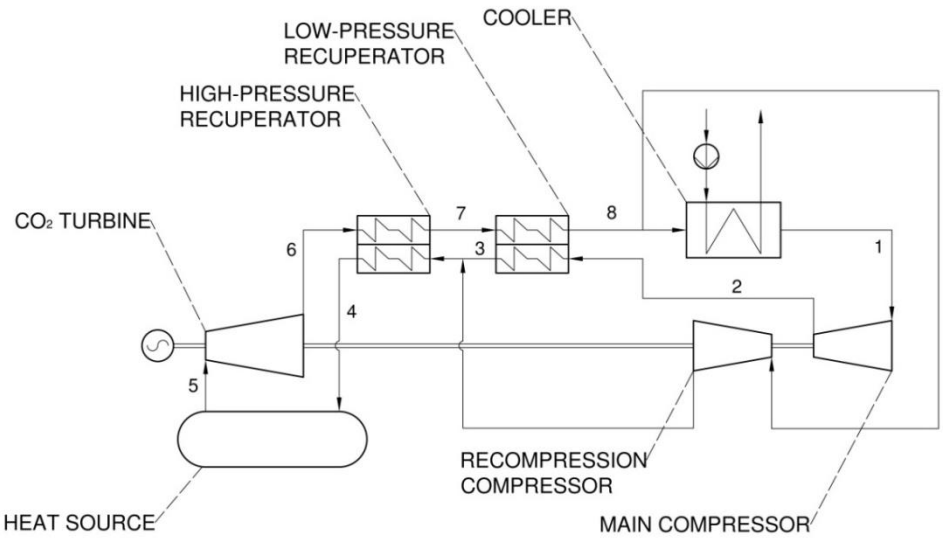

Figure 1: Scheme of the recompression supercritical CO_2 (s-CO_2) cycle

The s-CO_2 cycle, which was introduced by Feher [36], is a closed-loop Brayton cycle that is highly recuperative and operates entirely above CO_2 critical pressure [28], [36,38]. The heat capacity of supercritical CO_2 varies substantially with pressure [29],

and thus the simple s-CO_2 cycle suffers from large irreversibility in the recuperator caused by the heat capacity imbalance between its hot and cold sides [35]. This causes a pinch point problem in the recuperator [31,35] that is reflected in the minimum temperature approach occurring inside the heat exchanger [34]. In the recompression s-CO_2 cycle (Figure 1), which is considered in this study, this issue is resolved through recompressing part of the CO_2 stream without heat rejection to compensate the heat capacity difference in a low-temperature recuperator (LTR) [29]. As a result of increased LTR effectiveness, the hot stream enters a high-temperature recuperator (HTR) at a higher temperature. This, in turn, increases the temperature of the hot stream leaving the HTR and thus the average temperature of heat addition, leading to higher cycle efficiency [28].

2.2 Supercritical coal-fired power plant

A process model of a 580 MW_{el} supercritical coal-fired power plant, which is considered as a benchmark in this study, was developed in Aspen Plus and described in detail by Hanak et al. [25,54]. The prediction of this model was found to be in close agreement with data provided in the revised NETL report [55], confirming the efficacy of the modelling approach and high fidelity of the model.

The coal-fired power plant model comprises three sub-models: supercritical boiler and flue gas treatment train (NO_x, SO_x and fly ash) models, both modelled using Peng–Robinson–Boston–Mathias (PR–BM) equation of state, as well as a steam cycle model that has been thermodynamically described with steam tables (STEAMNBS). Coal combustion is modelled using solid modelling features recommended by AspenTech [56]. The boiler heat exchange sections, which include the primary, secondary, and reheat superheaters, as well as the economiser, are modelled using *HEATX* block with pressure drops and temperature levels set based on the revised NETL report [55].

Steam turbines are modelled as individual turbine sections using *COMPR* block, hence the high-, intermediate- and low-pressure cylinders are further divided into the required steam turbine sections. The isentropic efficiency was estimated to match the desired discharge temperature of each section, which was provided in the revised NETL report [55]. The condenser is modelled as *HEATX* block and is assumed to operate at a fixed pressure of 0.069 bar, which corresponds to a condensation temperature of 38.7°C. The performance of the modelled coal-fired power plant is characterised by gross power output of 580.4 MW_{el}, net thermal efficiency of 38.5%$_{HHV}$ and other key performance parameters estimated by Hanak et al. [25] and presented in Table 1.

Table 1: Reference coal-fired power plant and CaL retrofit (supercritical steam cycle) operating specification

Parameter	Reference coal-fired power plant [25]	CaL retrofit (supercritical steam cycle) [45]
System performance indicators		
Gross power output (MW_{el})	580.4	1023.3
Net power output (MW_{el})	552.7	799.9
Net thermal efficiency(%$_{HHV}$)	38.5	30.6
Specific coal consumption ($g/kW_{el}h$)	350.3	438.2
Calcium looping specification		
Limestone make-up rate (F_0/F_R) (-)	-	0.04
Carbonator temperature (°C)	-	650
Calciner temperature (°C)	-	900
Oxygen content in calciner fluidising gas (%$_{vol,wet}$)	-	40
Excess oxygen (%$_{vol,dry}$)	-	2.5
Primary and secondary steam cycle specification		
Live steam pressure (bar)	242.3	
Reheated steam pressure (bar)	45.2	
Intermediate-/low-pressure crossover pressure (bar)	9.3	
Condenser pressure (bar)	0.069	
Live and reheated steam temperature (°C)	593.3	

2.3 Calcium looping plant with supercritical steam cycle

The process model of the CaL plant, which is modelled using SOLIDS property method, with a supercritical steam cycle was developed in Aspen Plus and described in detail in Hanak et al. [45]. The prediction of the CaL model showed good agreement with data available in the literature [57–60].

In the CaL model, the carbonation process is modelled using the *RSTOIC* block in conjunction with the maximum average sorbent conversion model derived by Rodríguez et al. [61] and presented in Eq. (1). The maximum average conversion in this model is a function of the carbonation (f_{carb}) and calcination extent (f_{calc}), sorbent characteristics (a_1, a_2, f_1, f_2, b), which were estimated based on experimental data from the 1.7 MW_{th} INCAR-CSIC pilot plant [57], fresh limestone make-up (F_0) and solids looping rate (F_R). The carbonation conversion and the CO_2 capture level, which are used to determine the solids looping rate, are estimated using Eq. (2) and Eq. (3), respectively.

$$\mathrm{X}_{ave} = \left(F_0 + F_R \frac{F_0(1-f_{calc})}{F_0 + F_R f_{calc}}\right) f_{calc} \left[\frac{a_1 f_1^2}{F_0 + F_R f_{carb} f_{calc}(1-f_1)} + \frac{a_2 f_2^2}{F_0 + F_R f_{carb} f_{calc}(1-f_2)} + \frac{b}{F_0}\right] \quad (1)$$

$$\Delta\mathrm{X}_{carb} = f_{calc} f_{carb} \mathrm{X}_{ave} \quad (2)$$

$$E_{CO_2} = \frac{F_R}{F_{CO_2}} \Delta\mathrm{X}_{carb} \quad (3)$$

The calcination process, which aims at regeneration of the saturated sorbent, is modelled using *RGibbs* block that determines the chemical and phase equilibrium through the Gibbs' free energy minimisation at a given temperature. The equilibrium limits of the carbonation and calcination processes are accounted for using the correlation derived by Baker [62] to estimate the equilibrium partial pressure of CO_2 in the gas streams leaving the reactors. Finally, the CaL plant model comprises the auxiliary units, such as conventional air separation unit (ASU) and CO_2 compression

unit (CCU), for which a detailed modelling approach is widely described in the literature [45,54,63–66].

In the retrofitted system operating with the characteristics presented in Table 1, which were identified in Hanak et al. [45], the high-grade heat from the CaL plant was utilised to generate high-pressure steam, which has the same parameters as the supercritical boiler (593.3°C/593.3°C/242.3 bar), for the secondary steam cycle of similar operating conditions to the primary steam cycle. Both the heat recovery steam generator (HRSG) and the secondary steam cycle were modelled using the same approach as adapted for the coal-fired power plant model. The analysis performed by Hanak et al. [45] revealed that retrofit of the CaL plant with supercritical steam cycle to the reference coal-fired power plant increased the net power output of the retrofitted system by 44.7% and resulted in 7.9%$_{HHV}$ points drop in its net efficiency (Table 1). The performance of the CaL plant with the supercritical steam cycle will be used to assess if application of the s-CO_2 cycle to recover the high-grade heat from the CaL plant will bring performance benefits.

2.4 Supercritical CO_2 cycle

2.4.1 Model description and verification

A process model of the recompression s-CO_2 cycle has been developed in Aspen Plus based on data from Moisseytsev and Sienicki [29], who analysed the integration of the s-CO_2 cycle with the reference 96 MW_{el} sodium-cooled fast reactor. One of the main technical challenges of the s-CO_2 cycle is estimation accuracy of the turbomachinery efficiencies [44], as these units are still under development and only a few have been tested at bench- and pilot-scale [42,67]. In the open literature, the performance of the CO_2 turbine is usually represented using its isentropic efficiency, the typical value of

which is between 87.0% and 93.4% [28,31,34,43,68,69]. Similarly, the performance of the main and the recompression compressors is represented by isentropic efficiency of 85.0–95.5% [28,31,34,43,44].

Table 2: Reference recompression supercritical CO_2 cycle operating parameters

Parameter	Value
Main compressor discharge pressure (bar)	200.0
Recompression compressor discharge pressure (bar)	199.6
Turbine discharge pressure (bar)	77.3
Cycle lowest pressure (bar)	74.0
Cooler outlet temperature (°C)	31.3
Fraction of CO_2 to recompression (%)	29.0
Turbine isentropic efficiency (%)	93.0
Compressor isentropic efficiency (%)	90.0
Mechanical efficiency of the rotational machinery (%)	99.0
Generator efficiency (%)	98.5

Table 3: Benchmark of the supercritical recompression CO_2 cycle stream data with Moisseytsev and Sienicki [29]

Stream	Temperature (°C)		Pressure (bar)	
	Literature	Model	Literature	Model
1	31.3	31.3	74.0	74.0
2	84.4	82.8	200.0	200.0
3	171.8	171.8	199.6	199.6
4	323.3	323.3	199.1	199.1
5	471.8	471.5	198.4	198.4
6	362.3	361.8	77.3	77.3
7	190.7	189.0	76.9	76.9
8	90.2	87.7	76.3	76.3

Using the parameters presented in Table 2, which were taken from Moisseytsev and Sienicki [29] and Le Moullec [44], the Lee-Kesler-Plocker equation of state [44], the *HEATX* blocks to represent performance of the LTR, HTR and cooler, and the *COMPR* blocks to represent performance of the CO_2 turbines and compressors, the net efficiency of the cycle presented in Figure 1 is estimated to be 39.6%, which is 0.8% points lower than that of the reference study [29]. The main reason for such deviation

is the fact that the isentropic efficiencies for the CO_2 turbine and compressors were not provided in the reference study [29] and thus were taken from Le Moullec [44], who used the same reference system in his study. This is reflected in small deviations in prediction of the temperatures for the steams leaving the main compressor and the CO_2 turbine (Table 3). Nevertheless, the model prediction was found to be in good agreement with the literature data as the highest relative error was 2.8%.

2.4.2 Adaptation of supercritical CO_2 cycle to calcium looping

A large fraction of the high-grade heat needs to be recovered from the flue gas and pure CO_2 streams leaving the CaL plant. The recompression s-CO_2 cycle shown in Figure 1 cannot, therefore, be directly integrated with CaL because the sensible heat of the process streams below 500°C would not be utilised in the system, leading to high energy losses. The same issue was encountered by Le Moullec [44], who analysed the implementation of the recompression s-CO_2 cycle in place of the steam cycle in the coal-fired power plant with an amine scrubbing CO_2 capture plant. This study showed that the low-grade heat can be recovered from the process streams by extracting part of the CO_2 stream leaving the main CO_2 compressor at low temperature and returning it after the HTR. The same approach is applied in this study (Figure 2) and the low-grade heat from the clean flue gas stream is recovered by cooling it to 60.0°C using around 15–17% of the CO_2 flow leaving the main compressor at 44.4°C. Moreover, heat carried with the CO_2 stream at 900°C is first used to superheat the CO_2 stream to the desired high-pressure turbine inlet temperature, and then to preheat the flue gas and the O_2 streams entering the CaL plant.

To maximise the CaL excess heat utilisation and the efficiency of the recompression s-CO_2 cycle, a single reheat and a single intercooling stage are considered in the base configuration. In this configuration, the high-pressure and the intermediate-pressure

turbine inlet temperature is 593.3°C. In addition, the high-pressure turbine inlet pressure is set as 242.3 bar and both turbine stages operate with constant pressure ratio. Such assumptions for the base configuration allow its direct comparison with the reference configuration, in which the excess heat from CaL is utilised in the supercritical reheated steam cycle. Design of the heat exchanger network is based on the assumption that the minimum temperature approach of the heat exchangers is 10°C [70], with exception of recuperators and superheaters/reheaters for which the minimum temperature approach of 5°C [31], [32] and 25°C [70], respectively, is used. Finally, the reported values for the mechanical efficiency of the turbomachinery and the electric efficiency of the generator vary between 99.6–100.0% [28,70] and 97.5%–98.5% [29,55,70], respectively. In this study the mechanical efficiencies of 99.8% and 99.6% are selected for CO_2 turbines and compressors, respectively, while the electric efficiency of 98.0% is chosen for the generator. The key design parameters for the recompression s-CO_2 cycle adapted to the CaL plant are summarised in Table 4.

Table 4: Design basis for the recompression supercritical CO_2 cycle

Parameter	Value
Isentropic efficiency of CO_2 turbines (%)	93.0
Isentropic efficiency of main compressors (%)	90.0
Isentropic efficiency of recompression compressor (%)	90.0
Mechanical efficiency of CO_2 turbines (%)	99.8
Mechanical efficiency of compressors (%)	99.6
Electric generator efficiency (%)	98.0
Reheater and superheater minimum temperature approach (°C)	25.0
Heat exchangers minimum temperature approach (°C)	10.0
Recuperators minimum temperature approach (°C)	5.0
Heat exchanger pressure drop (%)	2.0

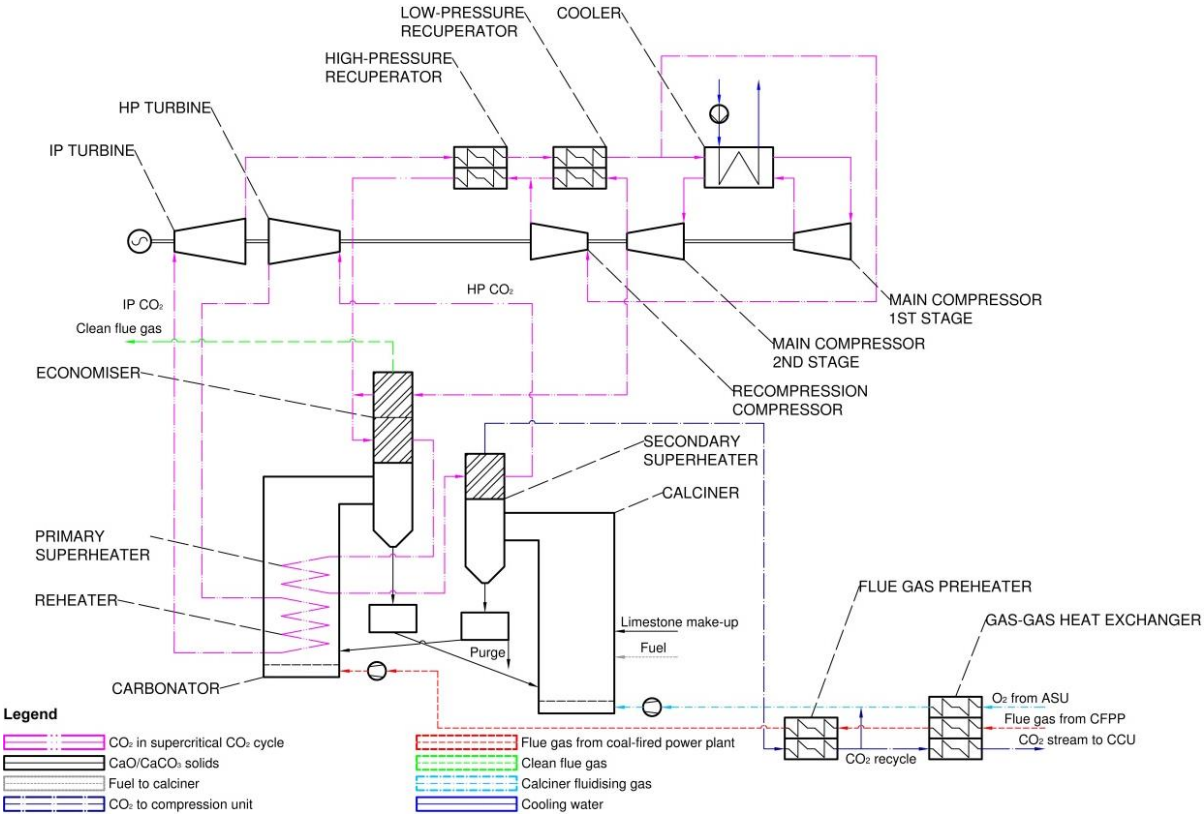

Figure 2: Scheme of the calcium looping process integrated with the recompression supercritical CO_2 cycle

3 PROCESS ANALYSIS

3.1 Considerations

Having adapted the recompression s-CO_2 cycle to recover the excess heat from the CaL plant, the retrofitted system needs to be benchmarked with the systems currently considered as state of the art. Therefore, the performance of the base configuration is compared with the CaL plant integrated with the supercritical reheated steam cycle. The comparison is made to the best configuration from Hanak et al. [45] in which oxy-combustion of coal is used to provide heat for sorbent regeneration in the calciner. Moreover, in both configurations, the CaL plant is retrofitted to the 580 MW_{el} supercritical coal-fired power plant to achieve the total CO_2 capture level of 90%.

A common feature of each Brayton cycle is the fact that the cycle efficiency can be further improved by introducing more reheat and intercooling stages, which would

increase the average temperature of heat addition and decrease the average temperature of heat rejection, respectively. Despite additional cost associated with the additional equipment, such designs would allow for more compact design of reheaters and intercoolers [44]. Dostal et al. [34] have estimated that the first reheat stage results in about 1.2% points improvement in the s-CO_2 cycle efficiency, while the second reheat stage adds only about 0.5% points to the efficiency. Their study also revealed that intercooling can increase the s-CO_2 cycle efficiency by up to 0.8% points. Although introducing more than one reheat and intercooling stage may not be an economically attractive option [34], it is worth exploring their effect on the net efficiency of the retrofitted system. Moreover, the fact that CO_2 is above its supercritical pressure (74 bar) throughout the cycle allows turning it to the dense phase by cooling it below the critical temperature (31.3°C). As a result, a pump can be used in place of the main compressor to increase the CO_2 pressure. Therefore, the following cases are considered in the configuration sensitivity study:

- Effect of reheat considering up to three expansion stages.
- Effect of intercooling by considering up to three compression stages.
- Effect of using a pump instead of the main compressor.

The performance of each thermodynamic cycle can be improved by increasing the operating temperature and pressure at the turbine inlet. Therefore, another sensitivity analysis is conducted to assess the effect of the high-pressure turbine inlet pressure and temperature on the net efficiency of the retrofitted system by varying the pressure between 200–300 bar and the temperature between 540–640°C. Finally, by combining both sensitivity studies the performance of the optimum design is estimated.

Table 5: Comparison of the key performance indicators

Parameter	Reference coal-fired power plant [25]	CaL retrofit (supercritical steam cycle) [45]	CaL retrofit (s-CO_2 cycle)
System performance indicators			
Gross power output (MW_{el})	580.4	1023.3	1024.3
Total auxiliary electricity consumption (MW_{el})	27.7	223.5	217.9
Net power output (MW_{el})	552.7	799.9	806.4
Gross thermal efficiency ($\%_{HHV}$)	40.4	39.2	40.1
Net thermal efficiency ($\%_{HHV}$)	38.5	30.6	31.6
Net specific chemical energy consumption (kW_{ch}/kW_{el})	2.6	3.3	3.2
Specific coal consumption ($g/kW_{el}h$)	350.3	438.2	425.4
Integration impact indicators			
Increase in the net power output (%)	-	44.7	45.9
Net efficiency penalty ($\%_{HHV}$ points)	-	7.9	6.9
Increase in net specific chemical energy consumption (%)	-	26.9	23.1
Carbonator CO_2 capture level (%)	-	79.6	80.0
Total CO_2 capture level (%)	0.0	90.0	90.0
CO_2 intensity factor ($g/kW_{el}h$)	792.3	111.6	108.7

3.2 Performance evaluation

Analysis of the retrofit of the 580 MW_{el} coal-fired power plant with CaL plant using either the recompression s-CO_2 cycle or the supercritical steam cycle for excess heat recovery (Table 5) revealed that the gross and the net power output in both configurations were comparable and only slightly higher for the former cycle. Nevertheless, the net efficiency of the CaL integrated with the recompression s-CO_2 cycle was found to be 1%$_{HHV}$ point higher for the same high-pressure turbine inlet conditions. This is not only the result of a higher degree of high-grade heat utilisation in the recompression s-CO_2 cycle, but also due to more heat recovered to preheat the flue gas and the O_2 streams entering the CaL plant, which resulted in 2.9% reduction of the specific coal consumption of the retrofitted system (4.7% reduction of the coal

consumption in the calciner). As the specific capital cost ($/MW$_{el}$) of the s-$CO_2$ cycle has been estimated to be up to 27% lower than that of the supercritical steam cycle operating in the same envelope [34], the recompression s-CO_2 cycle can be considered as a technically and economically viable option for decarbonisation of coal-fired power plants using CaL.

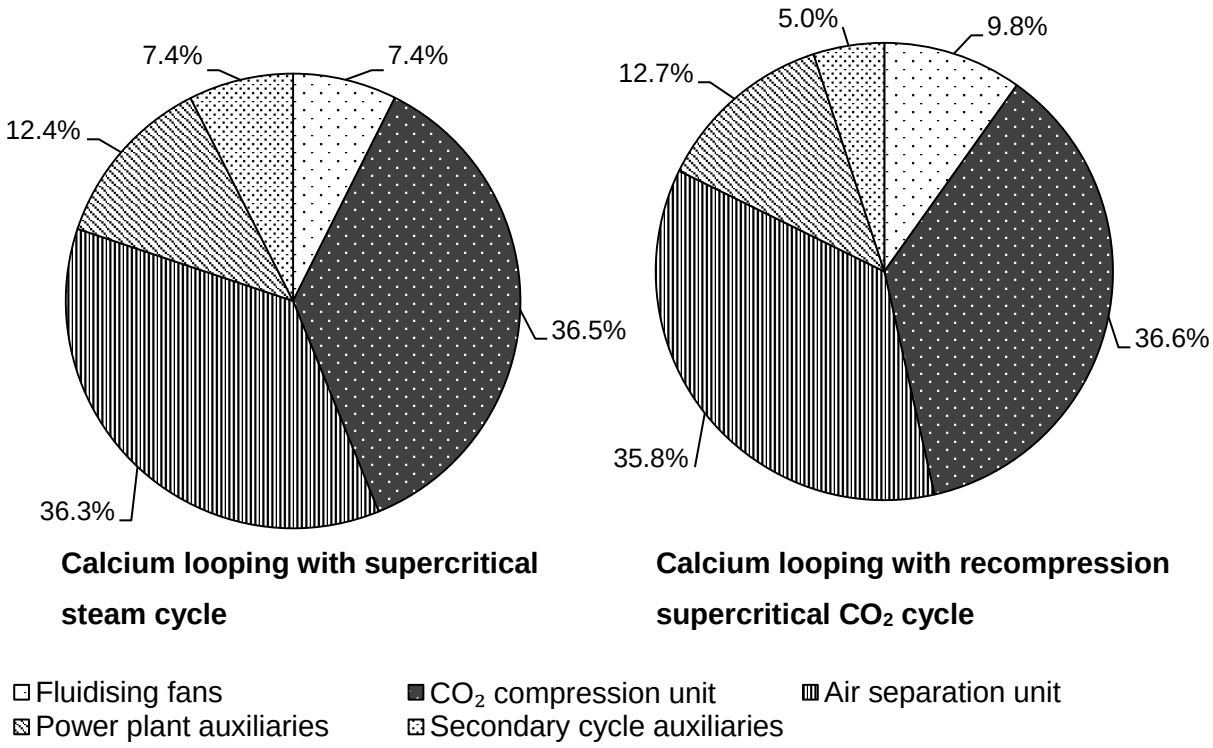

Figure 3: Effect of the calcium looping secondary thermodynamic cycle selection on a parasitic load distribution for the 580 MW$_{el}$ coal-fired power plant retrofit scenario

Analysing the distribution of the parasitic load (Figure 3), which again was estimated to be only slightly lower for the recompression s-CO_2 cycle, it is worth pointing out that the power requirement to run the ASU and the CCU compressors accounted for around 72.5% of the total system power requirement for both investigated configurations. As the remaining part of the parasitic load can be considered as unavoidable, further improvement of the retrofitted system's performance can be achieved through a more efficient secondary cycle, higher level of heat integration in the CaL plant, alternative O_2 sources, such as chemical looping combustion [71] or

membranes [72,73] for oxy-combustion of fuel or heat sources to sustain sorbent regeneration and alternative CO_2 compression options.

3.3 Recompression supercritical CO_2 cycle sensitivity study

3.3.1 Hardware analysis

The impact of the number of reheating and intercooling stages, as well as the kind of pressure-change equipment (compressors or pumps) is presented in Figure 4. It can be clearly seen that change in the hardware has a small effect on the parasitic load distribution, as the reduction in the gross efficiency associated with the power requirements of the particular components of the retrofitted system varies by up to 0.1%$_{HHV}$ points. Hence, improvement of the retrofitted system's performance is mostly associated with a higher cycle efficiency of the recompression s-CO_2 cycle.

The analysis revealed also that the net efficiency of the retrofitted system is more sensitive to the number of intercooling stages rather than to the number of reheating stages. Implementation of the first (T2C2) and the second (T3C2) reheat stage results in the net efficiency of the retrofitted system higher by 0.3%$_{HHV}$ points and 0.4%$_{HHV}$ points, respectively, with respect to the configuration without reheat (T1C2). Conversely, the net efficiency increase over the configuration without intercooling (T2C1) of 0.5%$_{HHV}$ points and 0.7%$_{HHV}$ points is reached on implementation of one (T2C2) and two (T2C3) intercooling stages, respectively. Hence, the base configuration with the single reheat and one intercooling stage appears to be an optimum one, as the addition of the second reheat and second intercooling stage results in net efficiency improvement of only 0.1%$_{HHV}$ points and 0.2%$_{HHV}$ points, respectively, and may not be economically viable. Importantly, the addition of intercooling allows reducing the clean flue gas temperature to 60°C, which is only

slightly above the flue gas discharge temperature in the reference coal-fired power plant (57.2°C), from 108.9°C. As a result, more low-grade heat is recovered from the CaL plant and used for power generation.

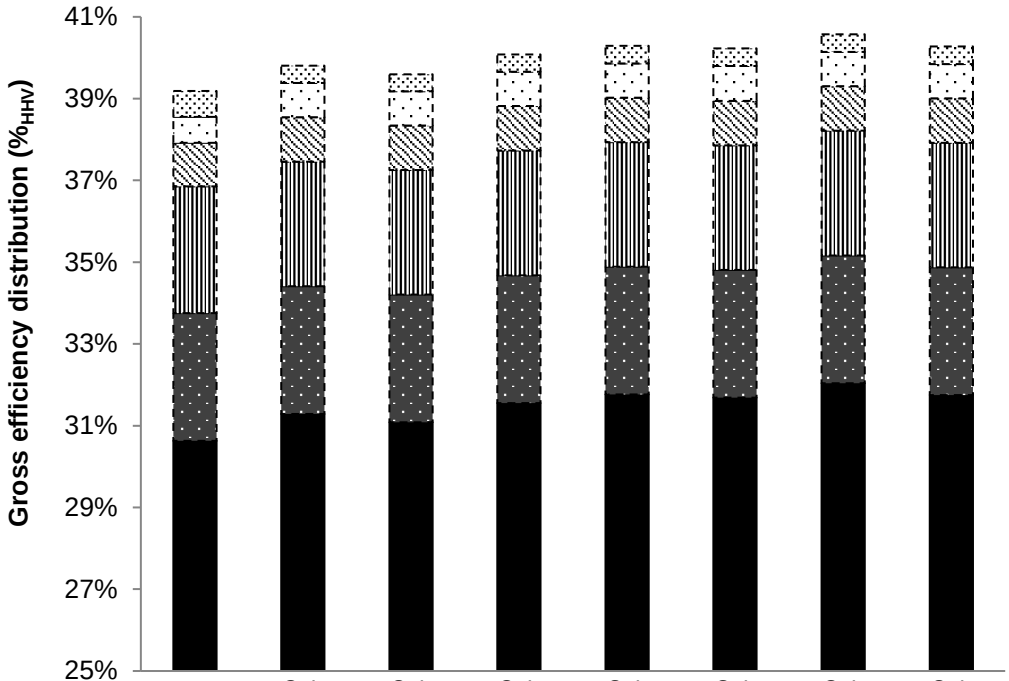

	CaL s-SC	CaL s-CO_2 (T1C2)	CaL s-CO_2 (T2C1)	CaL s-CO_2 (T2C2)	CaL s-CO_2 (T2C3)	CaL s-CO_2 (T3C2)	CaL s-CO_2 (T2C1P1)	CaL s-CO_2 (T2P2)
Secondary cycle auxilares	0.6%	0.4%	0.4%	0.4%	0.4%	0.4%	0.4%	0.4%
Fluidising fans	0.6%	0.8%	0.8%	0.8%	0.8%	0.9%	0.8%	0.8%
Power plant auxiliaries	1.1%	1.1%	1.1%	1.1%	1.1%	1.1%	1.1%	1.1%
Air separation unit	3.1%	3.1%	3.0%	3.1%	3.1%	3.0%	3.1%	3.1%
CO_2 compression unit	3.1%	3.1%	3.1%	3.1%	3.1%	3.1%	3.1%	3.1%
Net efficiency	30.6%	31.3%	31.1%	31.6%	31.8%	31.7%	32.0%	31.7%

Figure 4: Effect of recompression supercritical CO_2 cycle configuration on integrated process performance[a,b]

Additionally, implementation of one pump in place of the first compression stage in the base configuration (T2C1P1) resulted in a 0.4%$_{HHV}$ point increase, while substitution of both compression stages with pumps (T2P2) resulted in only 0.1%$_{HHV}$ point increase

[a] TxCyPz indicates number of turbine stages *x*, compression stages *y*, and pumping stages *z* in the configuration considered.
[b] CaL s-SC refers to the reference configuration in which the excess high-grade heat from CaL is recovered in the supercritical steam cycle, while CaL s-CO_2 refers to the configurations in which the excess high-grade heat from CaL is recovered in the recompression s-CO_2 cycle.

in the net thermal efficiency. This is because CO_2 is in the dense phase at the pump discharge, and thus enters the LTR at a lower temperature. The former configuration results in the highest net thermal efficiency of the retrofitted system, which is 32.0%$_{HHV}$ corresponding to an efficiency penalty of 6.4%$_{HHV}$ points.

3.3.2 Turbine inlet conditions analysis

As shown in Figure 5, increase in the net thermal efficiency of the retrofitted system is directly proportional to the increases in both the turbine inlet temperature and pressure. Yet, the maximum turbine inlet temperature (640°C) was limited by the assumption that the reheater outlet temperature is equal to the high-pressure turbine inlet temperature and the minimum temperature approach in the reheater of 10°C. Nevertheless, Dostal et al. [34] claimed that the recompression s-CO_2 cycle operating at the maximum temperature of 650°C and pressure higher than 200 bar is the most promising layout for the s-CO_2 cycle. Although increasing the turbine inlet temperature to 640°C was found to increase the net thermal efficiency to 32.1%$_{HHV}$, which corresponds to 6.4%$_{HHV}$ points drop from the reference value, it would require a large heat exchange area to reach the desired minimum temperature approach. Hence, a turbine inlet temperature of 620°C, which resulted in net thermal efficiency of 31.9%$_{HHV}$ and is the maximum temperature for the most advanced supercritical steam cycles [44], would be more suitable for short- to mid-term applications. Moreover, a maximum turbine inlet pressure of 300 bar was selected, because such pressures are allowed by a very-high-grade steel, which is required to allow for high-temperature operation and to prevent the system from corrosion induced by the flue gas components [44]. It was estimated that the retrofitted system with the recompression s-CO_2 cycle operating with such turbine inlet pressure had the net thermal efficiency of 31.9%$_{HHV}$.

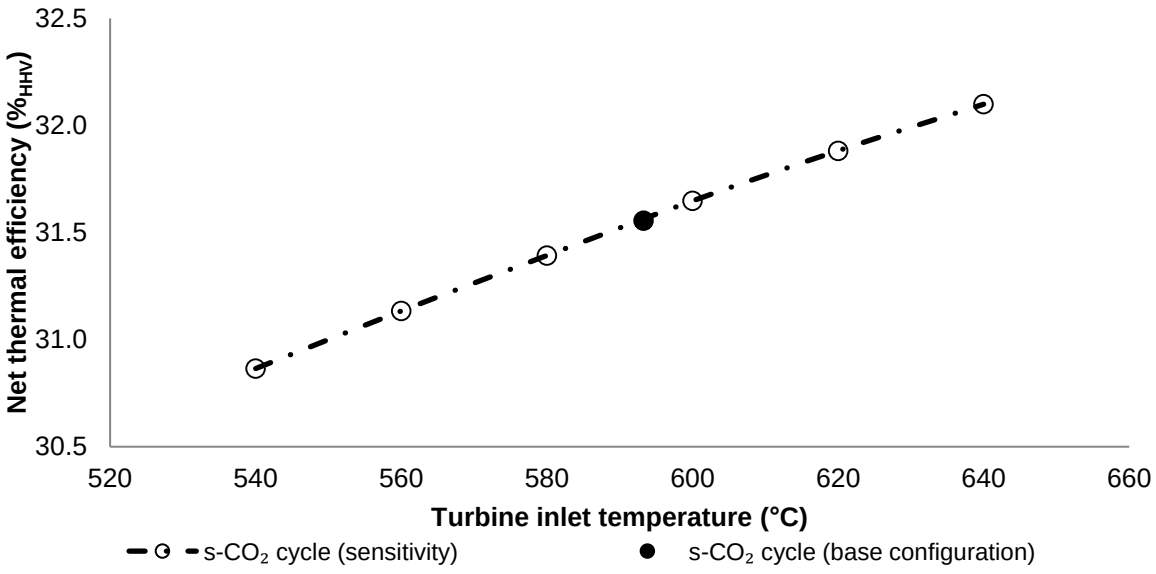

a)

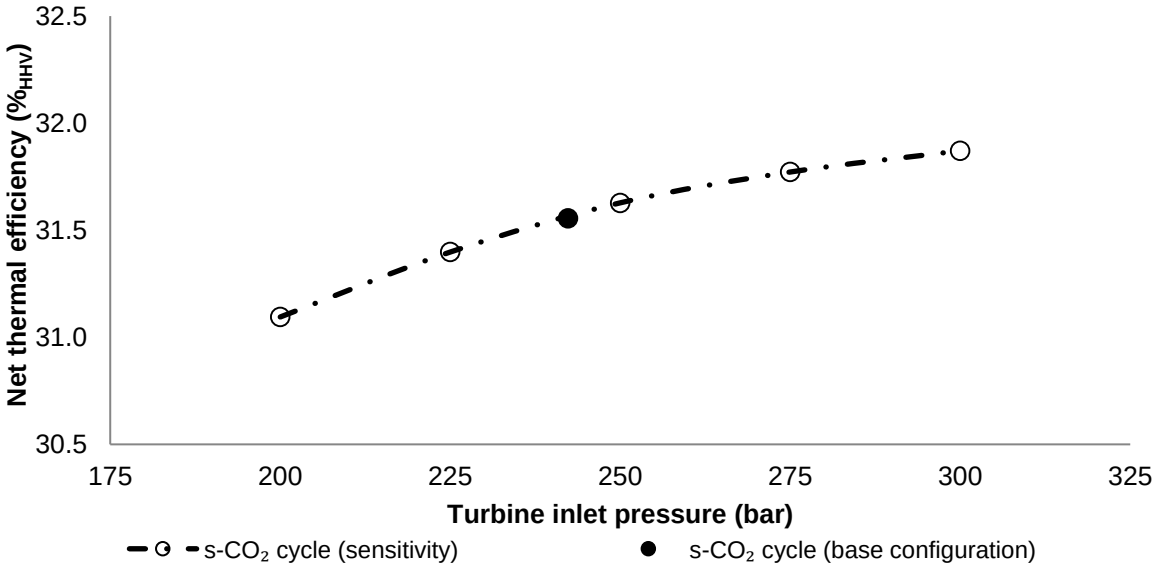

b)

Figure 5: Effect of turbine inlet a) temperature and b) pressure on the net thermal efficiency of the retrofitted system

Finally, it can be observed that the correlation with the temperature (Figure 5a) is nearly linear, while it is of second order for the pressure (Figure 5b). Such correlation for the latter parameter can be associated with the extent of the pressure drop in the heat exchangers, which increases with the cycle operating pressure. Analysis of the net thermal efficiency trends in Figure 5 indicated that further increase in the turbine inlet temperature, which would require a more complex heat exchanger network and

a multiple shaft turbine design, could result in an improvement of the process performance of about 0.1% per each 10°C increase in the turbine inlet temperature. On the contrary, increase in the turbine inlet pressure can be expected not to improve the net thermal efficiency of the retrofitted system much, mostly due to the associated increase in the pressure drop in the system.

3.3.3 Optimum recompression supercritical CO_2 cycle design

Having investigated how the performance of the retrofitted system varies with the recompression s-CO_2 cycle hardware and the turbine inlet conditions, the optimum configurations have been proposed and benchmarked against the base configuration in Table 6.

Table 6: Comparison of the key performance indicators for the optimised configurations

Parameter	Base case (T2C2)	Case 1 (T2C2)	Case 2 (T2C3)	Case 3 (T2C1P1)
Turbine inlet conditions				
Temperature (°C)	593.3	620.0	620.0	620.0
Pressure (bar)	300.0	300.0	300.0	300.0
System performance indicators				
Gross power output (MW_{el})	1024.3	1039.6	1045.7	1053.3
Net power output (MW_{el})	806.4	821.5	827.5	835.0
Gross thermal efficiency ($\%_{HHV}$)	40.1	40.8	41.0	41.3
Net thermal efficiency ($\%_{HHV}$)	31.6	32.2	32.4	32.7
Specific coal consumption ($g/kW_{el}h$)	425.4	416.9	413.9	410.1
Integration impact indicators				
Net efficiency penalty ($\%_{HHV}$ points)	6.9	6.3	6.1	5.8
CO_2 intensity factor ($g/kW_{el}h$)	108.7	106.5	105.7	104.7

It has been demonstrated in Section 3.3.2 that by increasing the turbine inlet temperature to 620°C, or increasing the pressure to 300 bar, the net thermal efficiency can increase by 0.3%$_{HHV}$ points. Unfortunately, no synergy effect occurred when both parameters were increased at the same time (Case 1), as the net thermal efficiency

identified in Table 6 increased by 0.6%$_{HHV}$ points over the base configuration, which is equal to the sum of increments incurred by a separate increase in the turbine inlet temperature and pressure. Moreover, allowing for higher capital cost, addition of the second intercooling stage (Case 2) improves the performance by another 0.2%$_{HHV}$ points, lowering the net efficiency penalty to 6.1%$_{HHV}$ points. Alternatively, by considering the pump in place of the first stage of the main compressor (Case 3), the retrofitted system performance can be improved by 0.5%$_{HHV}$ points, resulting in the net efficiency penalty of 5.8%$_{HHV}$ points. This corresponds to 1.1%$_{HHV}$ points improvement over the base configuration and 2.1%$_{HHV}$ points improvement over the best configuration for CaL with the supercritical steam cycle for coal-fired calciner reported by Hanak et al. [45].

4 CONCLUSIONS

This study proposed to use the recompression s-CO_2 cycle in place of the conventional steam cycle to recover high-grade heat from the CaL plant, which was retrofitted to the 580 MW_{el} supercritical coal-fired power plant. The recompression s-CO_2 was adapted to allow for a high degree of heat integration and to utilise the low-grade heat. The net efficiency of the base configuration, which was characterised by single reheat and intercooling stages (T2C2), was estimated to be 1.0%$_{HHV}$ points higher compared to the reference supercritical steam cycle under the same turbine inlet conditions.

Further improvements in the net efficiency of the retrofitted system were achieved by varying the hardware and the turbine inlet conditions. It was found that adding the second reheat (T3C2) and second intercooling (T2C3) resulted in 0.1%$_{HHV}$ and 0.2%$_{HHV}$ points increase in the net efficiency of the retrofitted system, respectively. Also, replacing the first stage of the main compressor (T2C1P1) with the pump was found to increase the net efficiency by 0.4%$_{HHV}$ points. Furthermore, it was found that

increase of the turbine inlet temperature and pressure to 640°C and 300 bar would increase the net efficiency of the retrofitted system to 32.1%$_{HHV}$ and 31.9%$_{HHV}$, respectively. However, considering the material availability and the short- to mid-term application of the proposed concept, the temperature of 620°C and pressure of 300 bar were selected for the optimal configurations. Depending on the hardware configuration, the net efficiency of the system can be increased to 32.2%$_{HHV}$ (T2C2), 32.4%$_{HHV}$ (T2C3) and 32.7%$_{HHV}$ (T2C1P1). The last configuration resulted in 2.1%$_{HHV}$ point net efficiency improvement over the reference CaL with the supercritical steam cycle (30.6%$_{HHV}$). As the specific capital cost of the s-CO_2 cycle is up to 27% lower than that of the equivalent steam cycle, this study proves the viability of the recompression s-CO_2 cycle application in CaL. Since the steam cycles for a high-grade heat recovery and power generation are integrated with other high-temperature looping cycles, such as chemical looping combustion, it can be expected that these can also benefit from the s-CO_2 cycle implementation.

The analysis revealed also that the performance of the coal-fired power plant retrofitted with the CaL plant, in which the excess heat is recovered in the recompression s-CO_2 cycle, can be further improved by:

- higher level of heat integration in the CaL plant, alternative sources of O_2 for oxy-combustion of fuel or sources of heat for sorbent regeneration to minimise or avoid the power requirement associated with O_2 production;
- alternative processes and technologies to minimise the power requirement for CO_2 compression prior to transport;
- higher efficiency of the secondary cycle, which for the recompression s-CO_2 cycle can be achieved through alternative configurations allowing increasing the turbine inlet temperature.

NOMENCLATURE

a_1	Sorbent average conversion model fitting parameter	-
a_2	Sorbent average conversion model fitting parameter	-
b	Sorbent average conversion model fitting parameter	-
F_0	Fresh limestone make up rate	kmol/s
f_1	Sorbent average conversion model fitting parameter	-
f_2	Sorbent average conversion model fitting parameter	-
E_{CO_2}	CO_2 capture level in the carbonator	-
F_{CO_2}	CO_2 flow rate entering the carbonator	kmol/s
F_R	CaO looping rate	kmol/s
f_{calc}	Calcination reaction extent	-
f_{carb}	Carbonation reaction extent	-
X_{ave}	Average sorbent conversion	-
ΔX_{carb}	Carbonation conversion	-

ABBREVIATIONS

ASU	Air separation unit
CaL	Calcium looping
CCS	Carbon capture and storage
CCU	CO_2 compression unit
HRSG	Heat-recovery steam generator
HTR	High-temperature recuperator
LTR	Low-temperature recuperator
s-CO_2	Supercritical CO_2 cycle

REFERENCES

[1] IPCC, *Climate Change 2007: The physical science basis: contribution of Working Group I to the Fourth Assessment Report of the Intergovernmental Panel on Climate Change,* Cambridge University Press, Cambridge, UK and New York, NY, USA, 2007.

[2] IPCC, *Climate change 2013. The physical science basic. Working group I contribution to the fifth assessment report of the Intergovernmental Panel on Climate Change*, Cambridge Unviersity Press, Cambridge, UK and New York, NY, USA, 2013.

[3] European Commission, *Communication from the Commission to the European Parliament, the Council, the European Economic and Social Committee and the Committee of the Regions - A Roadmap for moving to a competitive low carbon economy in 2050*, European Commission, Brussels, Belgium, 2011.

[4] IEA, *Tracking Clean Energy Progress 2013. IEA Input to the Clean Energy Ministerial*, IEA Publications, Paris, France, 2013.

[5] IEA, *Tracking Clean Energy Progress 2015. Energy Technology Perspectives 2015 Excerpt. IEA Input to the Clean Energy Ministerial*, IEA Publications, Paris, France, 2015.

[6] EIA, *Annual energy outlook 2015 with projections to 2040*, U.S. Energy Information Administration, Washington, DC, USA, 2015.

[7] O. Edenhofer, “King coal and the queen of subsidies”, *Science*, vol. 349, no. 6254, pp. 1286–1287, 2015.

[8] IEA, *Technology Roadmap: Carbon capture and storage*, IEA Publications, Paris, France, 2013.

[9] R. Stanger, T. Wall, R. Spörl, M. Paneru, S. Grathwohl, M. Weidmann, G. Scheffknecht, D. McDonald, K. Myöhänen, J. Ritvanen, S. Rahiala, T. Hyppänen, J. Mletzko, A. Kather, and S. Santos, “Oxyfuel combustion for CO_2 capture in power plants”, *International Journal of Greenhouse Gas Control*, vol. 40, pp. 55–125, 2015.

[10] Z. Liang, W. Rongwong, H. Liu, K. Fu, H. Gao, F. Cao, R. Zhang, T. Sema, A. Henni, K. Sumon, D. Nath, D. Gelowitz, W. Srisang, C. Saiwan, A. Benamor, M. Al-Marri, H. Shi, T. Supap, C. Chan, Q. Zhou, M. Abu-Zahra, M. Wilson, W. Olson, R. Idem, and P. Tontiwachwuthikul, “Recent progress and new developments in post-combustion carbon-capture technology with amine based solvents”, *International Journal of Greenhouse Gas Control*, vol. 40, pp. 26–54, 2015.

[11] G. Xu, H. G. Jin, Y. P. Yang, Y. J. Xu, H. Lin, and L. Duan, “A comprehensive techno-economic analysis method for power generation systems with CO_2 capture”, *International Journal of Energy Research*, vol. 34, no. 4, pp. 321–332, 2010.

[12] D. P. Hanak, C. Biliyok, H. Yeung, and R. Białecki, “Heat integration and exergy analysis for a high ash supercritical coal-fired power plant integrated with a post-combustion carbon capture process”, *Fuel*, vol. 134, pp. 126–139, 2014.

[13] H. M. Kvamsdal, M. C. Romano, L. van der Ham, D. Bonalumi, P. van Os, and E. Goetheer, “Energetic evaluation of a power plant integrated with apiperazine-based CO_2 capture process”, *International Journal of Greenhouse Gas Control*, vol. 28, no. 1, pp. 343–355, 2014.

[14] D. H. Van Wagener, U. Liebenthal, J. M. Plaza, A. Kather, and G. T. Rochelle, “Maximizing coal-fired power plant efficiency with integration of amine-based CO_2 capture in greenfield and retrofit scenarios”, *Energy*, vol. 72, pp. 824–831, 2014.

[15] M. E. Boot-Handford, J. C. Abanades, E. J. Anthony, M. J. Blunt, S. Brandani, N. Mac Dowell, J. R. Fernandez, M. C. Ferrari, R. Gross, J. P. Hallett, R. S. Haszeldine, P. Heptonstall, A. Lyngfelt, Z. Makuch, E. Mangano, R. T. J. Porter, M. Pourkashanian, G. T. Rochelle, N. Shah, J. G. Yao, and P. S. Fennell, “Carbon capture and storage update”, *Energy and Environmental Science*, vol. 7, pp. 130–189, 2014.

[16] Y. Hu, X. Li, H. Li, and J. Yan, “Peak and off-peak operations of the air separation unit in oxy-coal combustion power generation systems”, *Applied Energy*, vol. 112, pp. 747–754, 2013.

[17] A. S. Bhown and B. C. Freeman, “Analysis and status of post-combustion carbon dioxide capture technologies”, *Environmental Science and Technology*, vol. 45, no. 20, pp. 8624–8632, 2011.

[18] H. S. Kheshgi, H. Thomann, N. A. Bhore, R. B. Hirsch, M. E. Parker, and G. F. Teletzke, “Perspectives on CCS cost and economics”, *SPE Economics and Management,* vol. 4, no. 1, pp. 24–31, 2012.

[19] M. Renner, “Carbon prices and CCS investment: A comparative study between the European Union and China”, *Energy Policy*, vol. 75, pp. 327–340, 2014.

[20] CSIRO, *Assessing Post-Combustion Capture for Coal-fired Power Stations in Asia-Pacific Partnership Countries*, CSIRO Advanced Coal Technology, Newcastle, NW, USA, 2012.

[21] J. C. Abanades, B. Arias, A. Lyngfelt, T. Mattisson, D. E. Wiley, H. Li, M. T. Ho, E. Mangano, and S. Brandani, “Emerging CO_2 capture systems”, *International Journal of Greenhouse Gas Control*, vol. 40, pp. 126–166, 2015.

[22] T. Shimizu, T. Hirama, H. Hosoda, K. Kitano, M. Inagaki, and K. Tejima, “A Twin Fluid-Bed Reactor for Removal of CO_2 from Combustion Processes”, *Chemical Engineering Research and Design*, vol. 77, no. 1, pp. 62–68, 1999.

[23] D. P. Hanak, E. J. Anthony, and V. Manovic, “A review of developments in pilot plant testing and modelling of calcium looping process for CO_2 capture from power generation systems”, *Energy and Environmental Science.*, vol. 8, pp. 2199–2249, 2015.

[24] I. Martínez, R. Murillo, G. Grasa, and J. Carlos Abanades, “Integration of a Ca looping system for CO_2 capture in existing power plants”, *AIChE Journal*, vol. 57, no. 9, pp. 2599–2607, 2011.

[25] D. P. Hanak, C. Biliyok, and V. Manovic, “Rate-based model development, validation and analysis of chilled ammonia process as an alternative CO_2 capture technology for coal-fired power plants”, *International Journal of Greenhouse Gas Control*, vol. 34, pp. 52–62, 2015.

[26] S.-C. Yu, L. Chen, Y. Zhao, H.-X. Li, and X.-R. Zhang, “A brief review study of various thermodynamic cycles for high temperature power generation systems”,

Energy Conversion and Management., vol. 94, pp. 68–83, 2015.

[27] L. E. Herranz, J. I. Linares, and B. Y. Moratilla, “Power cycle assessment of nuclear high temperature gas-cooled reactors”, *Applied Thermal Engineering*, vol. 29, no. 8–9, pp. 1759–1765, 2009.

[28] J. Floyd, N. Alpy, A. Moisseytsev, D. Haubensack, G. Rodriguez, J. Sienicki, and G. Avakian, “A numerical investigation of the sCO_2 recompression cycle off-design behaviour, coupled to a sodium cooled fast reactor, for seasonal variation in the heat sink temperature”, *Nuclear Engineering and Design*, vol. 260, pp. 78–92, 2013.

[29] A. Moisseytsev and J. J. Sienicki, “Investigation of alternative layouts for the supercritical carbon dioxide Brayton cycle for a sodium-cooled fast reactor”, *Nuclear Engineering and Design*, vol. 239, no. 7, pp. 1362–1371, 2009.

[30] J. I. Linares, L. E. Herranz, I. Fernández, A. Cantizano, and B. Y. Moratilla, “Supercritical CO_2 Brayton power cycles for DEMO fusion reactor based on Helium Cooled Lithium Lead blanket”, *Applied Thermal Engineering*, vol. 76, pp. 123–133, 2015.

[31] R. V. Padilla, Y. C. Soo Too, R. Benito, and W. Stein, “Exergetic analysis of supercritical CO_2 Brayton cycles integrated with solar central receivers”, *Applied Energy*, vol. 148, pp. 348–365, 2015.

[32] C. S. Turchi, Z. Ma, T. W. Neises, and M. J. Wagner, “Thermodynamic Study of Advanced Supercritical Carbon Dioxide Power Cycles for Concentrating Solar Power Systems”, *Journal of Solar Energy Engineering*, vol. 135, no. 4, p. 041007, 2013.

[33] S. Wright, M. E. Vernon, and P. S. Pickard, *Concept design for a high temperature helium brayton cycle with interstage heating and cooling*, Sandia National Laboratories, Albuquerque, New Mexico and Livermore, California, 2006.

[34] V. Dostal, M. J. Driscoll, and P. Hejzlar, *A supercritical carbon dioxide cycle for next generation nuclear reactors*, Massachusetts Institute of Technology, Cambridge, MA, USA, 2004.

[35] H. S. Pham, N. Alpy, J. H. Ferrasse, O. Boutin, J. Quenaut, M. Tothill, D. Haubensack, and M. Saez, “Mapping of the thermodynamic performance of the supercritical CO_2 cycle and optimisation for a small modular reactor and a sodium-cooled fast reactor”, *Energy*, vol. 87, pp. 412–424, 2015.

[36] E. G. Feher, “The supercritical thermodynamic power cycle”, *Energy Conversion*, vol. 8, no. 2, pp. 85–90, 1968.

[37] G. Angelino, “Carbon dioxide condensation cycles for power production”, *ASME Journal of Engineering for Power*, vol. 90, no. 3, pp. 287–296, 1968.

[38] Y. M. Kim, C. G. Kim, and D. Favrat, “Transcritical or supercritical CO_2 cycles using both low- and high-temperature heat sources”, *Energy*, vol. 43, no. 1, pp. 402–415, 2012.

[39] D. Sánchez, R. Chacartegui, F. Jiménez-Espadafor, and T. Sánchez, “A new concept for high temperature fuel cell hybrid systems using supercritical carbon dioxide”, *Journal of Fuel Cell Science and Technology*, vol. 6, no. 2, p. 021306, 2009.

[40] Y. Song, J. Wang, Y. Dai, and E. Zhou, “Thermodynamic analysis of a transcritical CO_2 power cycle driven by solar energy with liquified natural gas as its heat sink”, *Applied Energy*, vol. 92, pp. 194–203, 2012.

[41] M. Liu, N. Lior, N. Zhang, and W. Han, “Thermoeconomic analysis of a novel zero-CO_2-emission high-efficiency power cycle using LNG coldness”, *Energy Conversion and Management.*, vol. 50, no. 11, pp. 2768–2781, 2009.

[42] B. D. Iverson, T. M. Conboy, J. J. Pasch, and A. M. Kruizenga, “Supercritical CO_2 Brayton cycles for solar-thermal energy”, *Applied Energy*, vol. 111, pp. 957–970, 2013.

[43] J. Sarkar and S. Bhattacharyya, “Optimization of recompression s-CO_2 power cycle with reheating”, *Energy Conversion and Management*, vol. 50, no. 8, pp. 1939–1945, 2009.

[44] Y. Le Moullec, “Conceptual study of a high efficiency coal-fired power plant with CO_2 capture using a supercritical CO_2 Brayton cycle”, *Energy*, vol. 49, no. 1, pp. 32–46, 2013.

[45] D. P. Hanak, C. Biliyok, E. J. Anthony, and V. Manovic, “Modelling and comparison of calcium looping and chemical solvent scrubbing retrofits for CO_2 capture from coal-fired power plant”, *International Journal of Greenhouse Gas Control*, vol. 42, pp. 226–236, 2015.

[46] J. C. Abanades, E. J. Anthony, J. Wang, and J. E. Oakey, “Fluidized Bed Combustion Systems Integrating CO_2 Capture with CaO”, *Environmental Science and Technology*, vol. 39, no. 8, pp. 2861–2866, 2005.

[47] L. M. Romeo, J. C. Abanades, J. M. Escosa, J. Paño, A. Giménez, A. Sánchez-Biezma, and J. C. Ballesteros“, Oxyfuel carbonation/calcination cycle for low cost CO_2 capture in existing power plants”, *Energy Conversion and Management*, vol. 49, no. 10, pp. 2809–2814, 2008.

[48] I. Vorrias, K. Atsonios, A. Nikolopoulos, N. Nikolopoulos, P. Grammelis, and E. Kakaras, “Calcium looping for CO_2 capture from a lignite fired power plant”, *Fuel*, vol. 113, pp. 826–836, 2013.

[49] J. Ströhle, A. Lasheras, A. Galloy, and B. Epple, “Simulation of the carbonate looping process for post-combustion CO_2 capture from a coal-fired power plant”, *Chemical Engineering and Technology*, vol. 32, no. 3, pp. 435–442, 2009.

[50] A. Lasheras, J. Ströhle, A. Galloy, and B. Epple, “Carbonate looping process simulation using a 1D fluidized bed model for the carbonator”, *International Journal of Greenhouse Gas Control*, vol. 5, no. 4, pp. 686–693, 2011.

[51] Y. Lara, P. Lisbona, A. Martínez, and L. M. Romeo, “Design and analysis of heat exchanger networks for integrated Ca-looping systems”, *Applied Energy*, vol. 111, pp. 690–700, 2013.

[52] D. Berstad, R. Anantharaman, and K. Jordal, “Post-combustion CO_2 capture from a natural gas combined cycle by $CaO/CaCO_3$ looping”, *International Journal of Greenhouse Gas Control*, vol. 11, pp. 25–33, 2012.

[53] W. Wang, S. Ramkumar, and L. Fan, “Energy penalty of CO_2 capture for the Carbonation–Calcination Reaction (CCR) Process: Parametric effects and comparisons with alternative processes”, *Fuel*, vol. 104, pp. 561–574, 2013.

[54] D. P. Hanak, C. Biliyok, and V. Manovic, “Efficiency improvements for the coal-

fired power plant retrofit with CO_2 capture plant using chilled ammonia process", *Applied Energy*, vol. 151, pp. 258–272, 2015.

[55] J. Black, *Cost and Performance Baseline for Fossil Energy Plants Volume 1: Bituminous Coal and Natural Gas to Electricity*, National Energy Technology Laboratory, 2013.

[56] AspenTech, *Aspen Plus: Getting Started Modeling Processes with Solids*, Aspen Technology Inc, Burlington, MA, USA, 2013.

[57] A. Sánchez-Biezma, J. Paniagua, L. Diaz, M. Lorenzo, J. Alvarez, D. Martínez, B. Arias, M. E. Diego, and J. C. Abanades, "Testing postcombustion CO_2 capture with CaO in a 1.7 MW_t pilot facility", *Energy Procedia*, vol. 37, pp. 1–8, 2013.

[58] A. Sánchez-Biezma, J. C. Ballesteros, L. Diaz, E. de Zárraga, F. J. Álvarez, J. López, B. Arias, G. Grasa, and J. C. Abanades, "Postcombustion CO_2 capture with CaO. Status of the technology and next steps towards large scale demonstration", *Energy Procedia*, vol. 4, pp. 852–859, 2011.

[59] B. Arias, M. E. Diego, J. C. Abanades, M. Lorenzo, L. Diaz, D. Martínez, J. Alvarez, and A. Sánchez-Biezma, "Demonstration of steady state CO_2 capture in a 1.7MW_{th} calcium looping pilot", *International Journal of Greenhouse Gas Control*, vol. 18, pp. 237–245, 2013.

[60] A. Charitos, N. Rodríguez, C. Hawthorne, M. Alonso, M. Zieba, B. Arias, G. Kopanakis, G. Scheffknecht, and J. C. Abanades, "Experimental Validation of the Calcium Looping CO_2 Capture Process with Two Circulating Fluidized Bed Carbonator Reactors", *Industrial and Engineering Chemistry Research*, vol. 50, no. 16, pp. 9685–9695, 2011.

[61] N. Rodríguez, M. Alonso, and J. C. Abanades, "Average activity of CaO particles in a calcium looping system", *Chemical Engineering Journal*, vol. 156, no. 2, pp. 388–394, 2010.

[62] E. H. Baker, "The calcium oxide-carbon dioxide system in the pressure range 1-300 atmospheres", *Journal of the Chemical Society*, pp. 464–470, 1962.

[63] T. Sanpasertparnich, R. Idem, I. Bolea, D. de Montigny, and P.

Tontiwachwuthikul, “Integration of post-combustion capture and storage into a pulverized coal-fired power plant”, *International Journal of Greenhouse Gas Control*, vol. 4, no. 3, pp. 499–510, 2010.

[64] I. Pfaff, J. Oexmann, and A. Kather, “Optimised integration of post-combustion CO_2 capture process in greenfield power plants”, *Energy*, vol. 35, no. 10, pp. 4030–4041, 2010.

[65] S. Posch and M. Haider, “Optimization of CO_2 compression and purification units (CO_2CPU) for CCS power plants”, *Fuel*, vol. 101, pp. 254–263, 2012.

[66] AspenTech, *Aspen Plus IGCC Model*, Aspen Technology Inc., Burlington, MA, USA, 2011.

[67] S. A. Wright, R. F. Radel, M. E. Vernon, G. E. Rochau, and P. S. Pickard, *Operation and analysis of a supercritical CO_2 Brayton cycle*, Sandia National Laboratories, Albuquerque, New Mexico and Livermore, California, 2010.

[68] M. Utamura, “Thermodynamic analysis of part-flow cycle supercritical CO_2 gas turbines”, *Journal of Engineering for Gas Turbines and Power*, vol. 132, no. 11, pp. 111701(1–7), 2010.

[69] J. E. Cha, T. H. O. Lee, J. H. Eoh, S. H. Seong, S. O. Kim, D. E. Kim, K. Moohwan, T. W. Kim, and K. Y. Suh, “Development of a supercritical CO_2 brayton energy conversion system coupled with a sodium cooled fast reactor”, *Nuclear Engineering and Technology*, vol. 41, no. 8, pp. 1025–1044, 2009.

[70] R. Anantharaman, O. Bollard, N. Booth, E. van Dorst, C. Ekstrom, E. Sanchez Fernandes, F. Franco, E. Macchi, G. Manzolini, D. Nikolic, A. Pfeffer, M. Prins, S. Rezvani, and L. Robinson, *CArbon-free Electricity by SEWGS: Advanced materials, Reactor-, and process design. D 4.9 European best practice guidelines for assessment of CO_2 capture technologies*, Politecnico di Milano – Alstom UK, 2011.

[71] V. Manovic and E. J. Anthony, “Integration of calcium and chemical looping combustion using composite CaO/CuO-based materials”, *Environmental Science and Technology*, vol. 45, no. 24, pp. 10750–10756, 2011.

[72] W. Chen, L. van der Ham, A. Nijmeijer, and L. Winnubst, “Membrane-integrated

oxy-fuel combustion of coal: Process design and simulation", *Journal of Membrane Science*, vol. 492, pp. 461–470, 2015.

[73] M. Puig-Arnavat, M. Søgaard, K. Hjuler, J. Ahrenfeldt, U. B. Henriksen, and P. V. Hendriksen, "Integration of oxygen membranes for oxygen production in cement plants", *Energy*, vol. 91, pp. 852–865, 2015.